

CHAPTER-2

EXPERIMENTAL PROCEDURE

Experiments were performed to understand the interaction between the inhibitor molecules with N80 steel, mild steel and J55 steel in various acid solutions i.e. 15% (HCl), 20% H₂SO₄ and 3.5% NaCl saturated with CO₂ respectively.

2.1. Materials

2.1.1. Composition of Testing Material

The corrosion tests were performed on N80 steel, mild steel and J55 steel. The N80 steel used in Chapter 3 section 3.1 and 3.2 has following composition (wt. %)

Table 2.1 Composition of N80 steel (wt. %)

C	Mn	P	Si	S	Cr	Fe
0.31	0.92	0.010	0.19	0.008	0.2	Balance

The composition of mild steel and J55 steel used in Chapter 3 section 3.3 and 3.4 are given in Table 2.2 and 2.3, in wt. % respectively.

Table 2.2 Composition of mild steel (wt. %)

C	Mn	P	Si	S	Fe
0.17	0.37	0.010	0.20	0.03	Balance

Table 2.3 Composition of J55 steel (wt. %)

C	Mn	P	Si	S	Cr	Ni	Mo	Fe
0.24	1.1	0.103	0.22	0.004	0.5	0.28	0.021	Balance

2.2. Sample preparation

The dimensions of N80 steel, mild steel and J55 steel strips used for weight loss and electrochemical experiments are 5.0 cm× 2.5 cm× 0.2 cm and 2.0 cm× 1.0 cm× 0.025 cm respectively. The strips were polished using SiC abrasive papers having grades ranging from 600 to 1200, degreased with acetone and dried at room temperature. For electrochemical experiments 1 cm² area of sample strips was used for testing and remaining area was covered with araldite resin.

2.3. Preparation of test solutions

The test solution used for N80 steel was 15% (v/v) HCl and was prepared by diluting 35% analytical grade (AR) HCl with double distilled water.

The test solution used for mild steel was 20% (v/v) H₂SO₄ and was prepared by diluting 98% analytical grade (AR) H₂SO₄ with double distilled water.

The test solution for J55 steel was 3.5% NaCl saturated with CO₂ and was prepared by using analytical grade (AR) NaCl. This prepared 3.5% NaCl solution was saturated with CO₂.

2.4. Selected inhibitors for study

In the present study ten inhibitors were tested as corrosion inhibitors. Seven were synthesized using conventional and microwave techniques in the laboratory and three were purchased from Sigma Aldrich. The corrosion inhibition performance of these inhibitors was evaluated using weight loss, electrochemical impedance spectroscopy and potentiodynamic polarization methods on N80 steel, mild steel and J55 steel in 15% HCl, 20% H₂SO₄ and 3.5% NaCl saturated with CO₂ respectively. The effect of different substituents was also studied. The inhibitors studied in the present work are listed below:

(A) Naphthyridine derivatives (ANCs)

(1) 2-amino-4-(4-methoxyphenyl)-1,8-naphthyridine-3-carbonitrile (ANC-1)

(2) 2-amino-4-(4-methylphenyl)-1,8-naphthyridine-3-carbonitrile (ANC-2)

(3) 2-amino-4-(3-nitrophenyl)-1,8-naphthyridine-3-carbonitrile (ANC-3)

(B) Pyridine derivatives (ADP and AMP)

(1) 2-amino-6-(2,4-dihydroxyphenyl)-4-(4-methoxyphenyl)nicotinonitrile (ADP)

(2) 2-amino-4-(4-methoxyphenyl)-6-phenylnicotinonitrile (AMP)

(C) Isatin derivatives (TZs)

(1) 1-Benzylidene-5-(2-oxoindoline-3-ylidene) Thiocarbohydrazone (TZ-1)

(2) 1-(4-Methylbenzylidene)-5-(2-oxoindolin-3-ylidene) Thiocarbohydrazone
(TZ-2)

(D) Porphyrin derivatives (P1, P2 and P3)

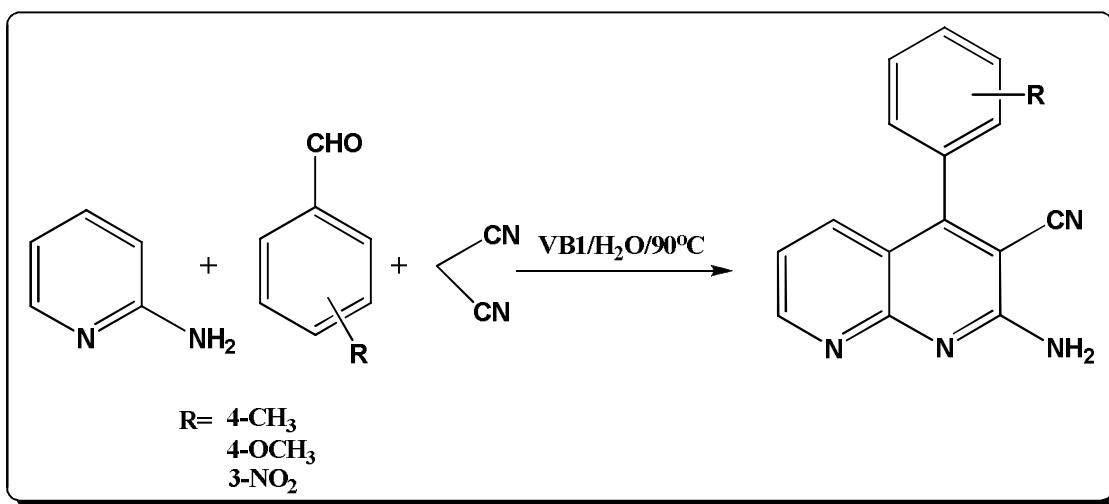
(1) 5,10,15,20-Tetra(4-pyridyl)- porphyrin (P1)

(2) 5,10,15,20-Tetraphenyl- porphyrin (P2)

(3) 5,10,15,20-Tetrakis(4-hydroxyphenyl)- porphyrin (P3)

2.4.1. Synthesis of Napthyridine derivatives [Siddiqui *et al.* (2013)]

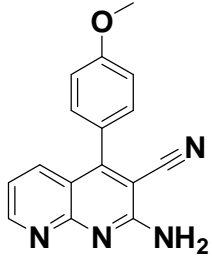
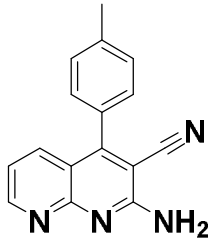
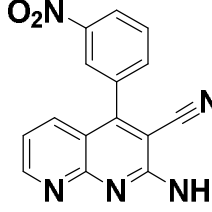
To a well-stirred solution of different aromatic aldehydes (10 mmol) and malononitrile (10 mmol) in presence of vitamin B1 (VB1) (10 mol %) in water (4 mL), 2-aminopyridine (10 mmol) was added and the reaction mixture was refluxed at 90 °C for 2-2.5 h time period. After completion of the reaction as monitored by TLC, the reaction mixture was cooled and the solid product was isolated by simple filtration. The products were purified by recrystallization from 95% ethanol.



Scheme-1: Synthesis of Napthyridine derivatives

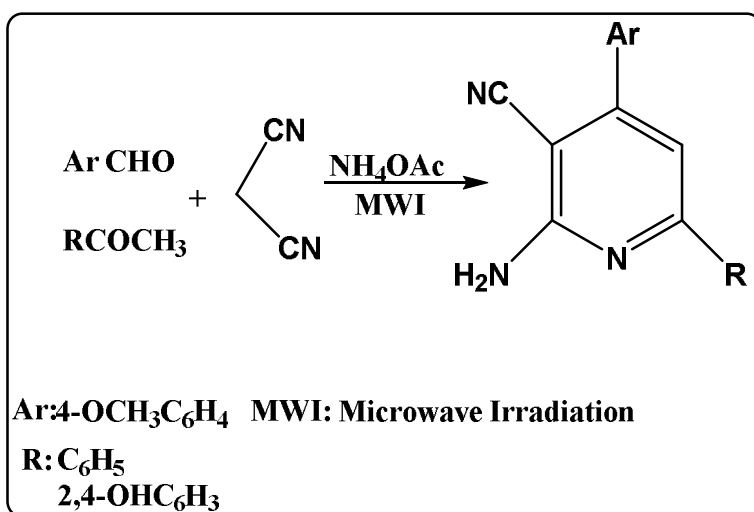
Table 2.4

The molecular structures, abbreviations, percentage yield, spectral data (IR and NMR data of a selected compound), IUPAC name and melting points of the synthesized Naphthyridine derivatives

IUPAC Name	Molecular Structure	Abbreviation	Yield (%)	Analytical data
2-amino-4-(4-methoxyphenyl)-1,8-naphthyridine-3-carbonitrile		ANC-1	95	MP: 158-160°C; IR (KBr, ν) 3240, 3281, 2230; ^1H NMR (400 MHz, DMSO): δ 3.84 (s, 3H), 6.89 (m, 2H, HAr), 7.27 (m, 1HAr), 7.33 (m, 1HAr), 7.35 (s, 2H, NH ₂), 7.39 (m, 2H, HAr), 7.43 (m, 1HAr)
2-amino-4-(4-methylphenyl)-1,8-naphthyridine-3-carbonitrile		ANC-2	94	MP: 156-158°C; IR (KBr, ν) 3252, 3290, 2241
2-amino-4-(3-nitrophenyl)-1,8-naphthyridine-3-carbonitrile		ANC-3	95	MP: 163°C; IR (KBr, ν) 3247, 3342, 2241

2.4.2. Synthesis of Pyridine derivatives [Shi *et al.* (2005)]

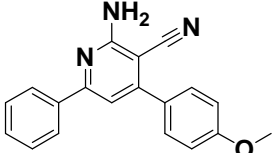
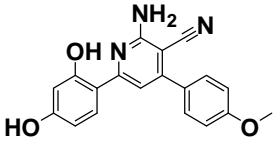
In a dry round bottom flask of 25 ml capacity, aldehyde (2 mmol), methyl ketone (2 mmol), malononitrile (2 mmol) and ammonium acetate (3 mmol) were added and placed in a microwave oven. This round bottom flask was then connected with refluxing equipment. After being irradiated for 7-9 min, the reaction mixture was washed with ethanol (2 mL). The crude products were purified by recrystallization from 95% ethanol to afford pure products.



Scheme-2: Synthesis of Pyridine derivatives

Table 2.5

The molecular structures, abbreviations, percentage yield, spectral data (IR and NMR data of a selected compound), IUPAC name and melting points of synthesized Pyridine derivatives

IUPAC Name	Molecular Structure	Abbreviation	Yield (%)	Analytical data
2-amino-4-(4-methoxyphenyl)-6-phenylnicotinonitrile		AMP	85	MP: 180-182°C; (KBr, ν) 3462 (N-H), 3184 (C-H, Ar), 2201 (CN); ¹ H NMR (400 MHz, DMSO): 8.11-8.12 (2H, m, ArH), 7.66 (2H, d, ArH), 7.48-7.49 (3H, m, ArH), 7.25 (1H, s, CH), 7.11 (2H, d, ArH), 6.96 (2H, s, NH ₂), 3.85 (3H, s, OCH ₃).
2-amino-6-(2,4-dihydroxyphenyl)-4-(4-methoxyphenyl)nicotinonitrile		ADP	89	MP: 188-190°C; (KBr, ν) 3453 (N-H), 3340 (O-H), 2218 (CN)

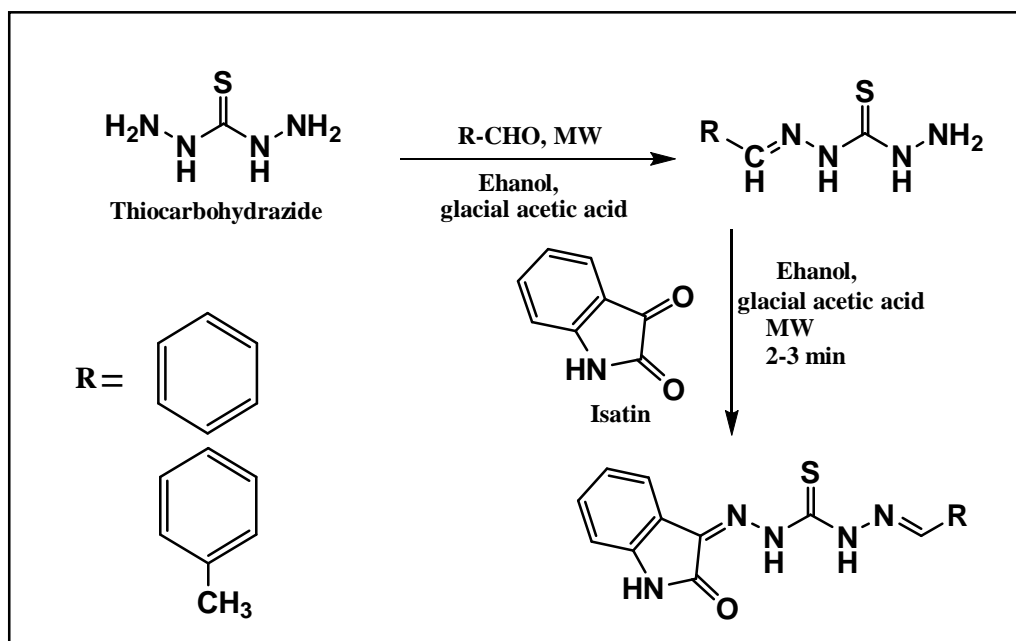
2.4.3. Synthesis of Isatin derivatives [Kiran *et al.* (2013)]

(a) Synthesis of Monothiocarbohydrazones:

In a round bottom flask thiocarbohydrazide (10 mmol) and substituted aldehyde (10 mmol) with catalytic amount of glacial acetic acid, and 20 ml ethanol were taken. The resulting mixture was irradiated under microwave for 10-12 min. After this the reaction mixture was cooled and the precipitate was collected by filtration. Further it was purified by recrystallization from ethanol.

(b) Synthesis of isatin Aldehyde-thiocarbohydrazones

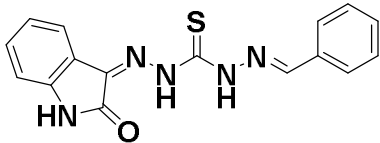
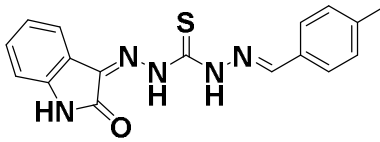
A mixture of monothiocarbohydrazone (10 mmol) and Isatin (10 mmol) with a catalytic amount of glacial acetic acid was taken in 30 mL of ethanol in a round bottom flask. Then the reaction mixture was irradiated under microwave for 10-12 mins. This reaction mixture was allowed to cool and the precipitate was collected by filtration.



Scheme-3: Synthesis of isatin derivatives

Table 2.6

The molecular structures, abbreviations, percentage yield, spectral data (IR and NMR data of a selected compound), IUPAC name and melting points of synthesized Isatin derivatives

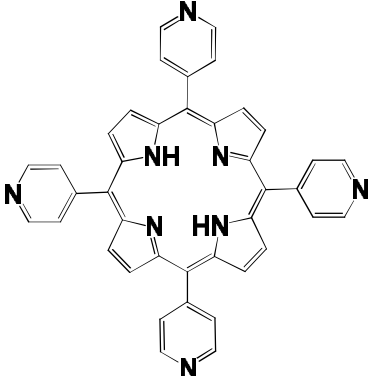
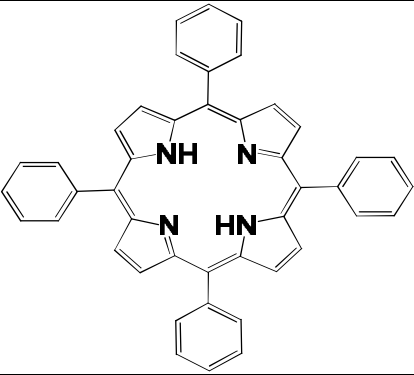
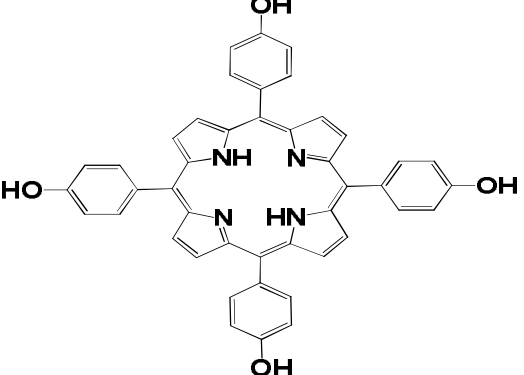
IUPAC Name	Molecular Structure	Abbri vation	Yield (%)	Analytical data
1-Benzylidene-5-(2-oxoindoline-3-ylidene) Thiocarbohydraz one		TZ-1	69	MP:230 232°C; IR (KBr, v): 3455 (N-H), 3140 (N-H), 3028 (C-H, Ar), 1693 (C=O), 1319 (C=S)
1-(4-Methylbenzylidene)-5-(2-oxoindolin-3-ylidene) Thiocarbohydraz one		TZ-2	75	MP: 228-230°C; IR (KBr, v): 3248 (N-H), 3010 (C-H, Ar), 1628 (C=O), 1306 (C=S); ¹ H-NMR (400 MHz DMSO) 13.4 (s, 1H), 12.3 (s, 1H), 10.1 (s, 1H), 7.95-7.88 (m, 3H), 7.68 (dd, 1H), 7.60 (dd, 1H), 7.48 (td, 1H), 7.43-7.37 (m, 2H), 7.27-7.20 (m, 1H), 2.41 (s, 3H)

2.4.4. Porphyrin derivatives

Porphyrins of analytical grade were purchased from Sigma Aldrich.

Table 2.7

The molecular structures, abbreviations of Porphyrin derivatives

IUPAC Name	Molecular Structure	Abbreviation
5,10,15,20-Tetra(4-pyridyl)-porphyrin	 The structure shows a central porphyrin ring with four nitrogen atoms. Each nitrogen is bonded to a hydrogen atom (NH or HN). The four meso positions of the porphyrin ring are substituted with 4-pyridyl groups, which are pyridine rings attached at their 4-position.	P1
5,10,15,20-Tetraphenylporphyrin	 The structure shows a central porphyrin ring with four nitrogen atoms. Each nitrogen is bonded to a hydrogen atom (NH or HN). The four meso positions of the porphyrin ring are substituted with phenyl groups, which are benzene rings attached at their 1-position.	P2
5,10,15,20-Tetrakis(4-hydroxyphenyl)-porphyrin	 The structure shows a central porphyrin ring with four nitrogen atoms. Each nitrogen is bonded to a hydrogen atom (NH or HN). The four meso positions of the porphyrin ring are substituted with 4-hydroxyphenyl groups, which are benzene rings with a hydroxyl group (-OH) at the 4-position.	P3

2.5. Tools

2.5.1 Characterization of Synthesized Compounds

(i) Melting point determination

Open capillaries were used for melting point determination.

(ii) Infrared spectroscopy and Nuclear magnetic resonance spectroscopy

Infrared (IR) spectra were recorded on KBr discs using Perkin Elmer (Spectrum100) Fourier transform (FT-IR) spectrophotometer. ¹H NMR (400 MHz) spectra were obtained by Bruker-NMR in DMSO using TMS as internal standard.

2.6. Techniques

2.6.1. Corrosion rate determination by weight loss study

N80 steel, mild steel and J55 steel strips used for weight loss experiments were cut into coupons with dimension of 5.0×2.5×0.2 cm, polished with SiC abrasive papers of grade 800-1200, cleaned with double distilled water and acetone, and finally dried. The total surface area of coupons was measured with accuracy by using the following equation [ASTM (1990)].

$$A = 2(lb + lt + bt - \pi r^2 + \pi rt)$$

t = thickness of a coupon (cm)

b = width of a coupon (cm)

l = length of a coupon (cm)

r = radius of the mounting hole

The cleaned and dried steel samples were weighed and immersed for a known period with the help of glass hooks in triplicate in 100 ml of corrosive solution in absence and in presence of the inhibitors [NACE (1987)]. The volume of the test solution was kept large enough to avoid any appreciable change in its corrosivity during the test, either through exhaustion of corrosive constituents or by accumulation of corrosion products that might

affect further corrosion [ASTM (2004)]. The effect of solution temperature and inhibitor concentration was varied with the purpose of the test. The temperatures of the experiments were maintained by using a digital thermostat. The steel samples were taken out from the corrosive solution after 6h time of immersion, washed in running water and finally washed with distilled water and dried in stream of warm air before weighing.

The corrosion rate C_R (mm/y), percentage inhibition efficiency (η %) and degree of surface coverage (θ) were determined by applying the following equations [ASTM (1987)]:

$$C_R (\text{mm / y}) = \frac{87.6 \times w}{ATD} \quad (2.1)$$

$$\eta \% = \frac{C_R^0 - C_R^i}{C_R^0} \times 100 \quad (2.2)$$

$$\theta = \frac{C_R^0 - C_R^i}{C_R^0} \quad (2.3)$$

where, w is the weight loss of the specimen (mg), A the surface area of a specimen (cm^2) D is density g/cm^3 , t is exposure time (h), C_R^0 and C_R^i are the weight loss values in absence and presence of inhibitor, respectively.

2.6.2. Electrochemical studies

Electrochemical studies were carried out by Gamry Instruments using three electrode assembly. N80, J55 and mild steel coupons with exposed area of 1 cm^2 were used as working electrodes. A Graphite rod and a saturated calomel electrode were used as counter and reference electrodes respectively. GAMRY Echem Analyst software package 5.0 was used for fitting impedance data in an equivalent circuit and also for extrapolating Tafel slopes. Prior to each experiment, steel samples were immersed in the corrosive medium in absence and presence of inhibitors for 30 min until a steady potential was reached.

(i) Electrochemical impedance spectroscopy

Electrochemical Impedance measurements were carried out in frequency range from 100 kHz to 0.5 Hz with amplitude of 10 mV peak to peak using AC signals vs open circuit potential. The Nyquist and Bode plots in absence and presence of inhibitors were obtained at 308 K. Different electrochemical parameters such as solution resistance (R_s), charge transfer resistance (R_{ct}), inductance (L), constant phase angle (CPE) and constants (Y_0 and n) were obtained by fitting equivalent circuits.

The impedance of the CPE can be given as follows [Yadav and Quraishi (2012 a)]:

$$Z_{CPE} = Y_0^{-1} (j\omega)^{-n}$$

where, Y_0 is the amplitude comparable to a capacitance, j is the square root of -1, ω is angular frequency and n is the phase shift. The values of the double layer capacitance (C_{dl}) and inhibition efficiency (η %) are calculated as follows [Yadav and Quraishi (2012 a)]:

$$C_{dl} = \frac{Y\omega^{n-1}}{\sin(n(\pi/2))} \quad (2.4)$$

$$\eta\% = \left(1 - \frac{R_{ct}}{R_{ct(i)}}\right) \times 100 \quad (2.5)$$

where, ω is the angular frequency ($\omega = 2\pi f_{max}$) at which the imaginary part of impedance ($-Z_{im}$) is maximal and n is the phase shift, R_{ct} and $R_{ct(i)}$ respectively represent the charge transfer resistance in absence and presence of inhibitors.

(ii) Potentiodynamic polarization

Potentiodynamic polarization curves were obtained by changing the electrode potential automatically from -250 to +250 mV at open circuit potential with a scan rate of 0.5 mV s⁻¹. Various electrochemical parameters, i.e., corrosion potential (E_{corr}), corrosion current density (I_{corr}), anodic Tafel slopes (β_a), cathodic Tafel slopes (β_c) and inhibition

efficiency (η %) were calculated. The η % was calculated using the following equation [Yadav and Quraishi (2012 a)]:

$$\eta \% = \left(1 - \frac{I_{\text{corr}(i)}}{I_{\text{corr}}} \right) \times 100 \quad (2.6)$$

where, I_{corr} and $I_{\text{corr}(i)}$ are the corrosion current densities obtained in absence and presence of inhibitor respectively.

2.7. Thermodynamic parameters determination

(i) Activation Energy:

Activation energy was determined by using equation [Yadav and Quraishi (2012 a)]:

$$C_R = A \exp\left(\frac{-E_a}{RT}\right) \quad (2.7)$$

where E_a is activation energy, R is the gas constant, A is the pre-exponential factor. The values of E_a can be calculated from the slopes of straight lines, which are obtained by plotting $\log C_R$ versus $1/T$.

(ii) Free Energy of Adsorption

The free energy of adsorption of inhibitor was calculated using the equation given below [Chidiebere *et al.* (2014)]:

$$\Delta G_{\text{ads}}^0 = -RT \ln(55.5K_{\text{ads}}) \quad (2.8)$$

and K_{ads} is given by:

$$K_{\text{ads}} = \frac{\theta}{1-\theta} \times \frac{1}{C_{\text{inh}}} \quad (2.9)$$

2.8. Scanning Electron Microscopy (SEM)

The surface morphology of the steel samples in absence and in presence of the inhibitors was studied by SEM using model Ziess Evo 50 XVP, at an accelerating voltage of 5 kV and magnification of 5kx. In this study, the steel samples of dimensions 5.0 cm ×

2.5 cm × 0.2 cm were immersed in the corrosive solution in absence and presence of optimum concentration of inhibitors for 6h. After this the steel samples were taken out, washed with distilled water, dried and mechanically cut into 1cm² size and were used for surface analysis.

2.9. Energy dispersive X-ray Spectroscopy (EDX)

The elemental composition of the adsorbed inhibitor film over the steel surface was examined by energy dispersive X-ray spectroscopy (EDX) which is coupled with SEM.

2.10. Contact angle measurements

Contact angle measurements were done using sessile drop technique on DSA100 Kruss instrument made in Germany.

2.11. Scanning Electrochemical Microscopy (SECM)

SECM was performed using model CHI900C. A 10 μm platinum tip was used as the probe, Ag/AgCl/KCl (saturated) and platinum were used as reference and counter electrodes respectively. All potential values were measured with respect to Ag/AgCl/KCl (saturated) reference electrode. The tip carried out the line scan measurements at the scan rate of 80 μm/step, which is at ~ 10 μm from the specimen surface.

2.12. Quantum chemical calculations

Gaussian 03-program package was used for all Quantum chemical calculations [Frisch *et al* (2007)]. DFT (B3LYP) optimized the molecular structures of inhibitors, in combination with the 6-31G (d, p) basis set. The following quantum chemical indices were taken into consideration: energy of the highest occupied molecular orbital (E_{HOMO}), energy of the lowest unoccupied molecular orbital (E_{LUMO}) and energy gap: $\Delta E = E_{\text{LUMO}} - E_{\text{HOMO}}$. All calculations were carried both on neutral and protonated molecules.

Molecular dynamic simulation (MD) was performed using Forcite module in the Material Studio Software 7.0 from BIOVIA-Accelrys, USA [Obot and Gasem (2014), Tan *et al.* (2015)]. The simulation was carried out with Fe (110) crystal with a slab of 5 Å in depth with periodic boundary conditions in order to simulate a representative part of an interface devoid of any arbitrary boundary effects. The Fe (110) plane was next enlarged to a (10 × 10) supercell to provide a large surface for the interaction of the inhibitors. After that, a vacuum slab with 30 Å thickness was built above the Fe (110) plane. The Fe (110) surface was fixed before simulations. For the whole simulation procedure, the Condensed-phase Optimized Molecular Potentials for Atomistic Simulation Studies (COMPASS) force field was used to optimize the structures of all components of the system of interest. The MD simulations were performed in NVT canonical ensemble at 298 K with a time step of 1.0 fs and a total simulation time of 500 ps using Anderson thermostat.